Review Article

Megha Choudhary, Aaruni Sharma, S. Aravind Raj*, Mohamed Thariq Hameed Sultan*, David Hui, and Ain Umaira Md Shah

Contemporary review on carbon nanotube (CNT) composites and their impact on multifarious applications

https://doi.org/10.1515/ntrev-2022-0146
received December 25, 2021; accepted April 5, 2022

Abstract: Since their discovery in 1991, carbon nanotubes (CNTs) have found widespread use in various industries, from aerospace to energy, due to their excellent mechanical, thermal, electrical, and tribological properties. Their lightweight nature, small size, incredible tensile strength, and conductivity have made them very popular as reinforcements in metals, polymers, and even finding employment in additive manufacturing. In this review, we provide a rundown of these structures and discuss in detail the numerous methods used to process CNT-reinforced materials, such as chemical vapor deposition (CVD), ball milling, hot pressing, and selective laser melting. The limitations of manufacturing and processing these composites are also discussed, strengthened by the support of different published works. To understand the changes in the properties of these composites in terms of varying parameters such as temperature, CNT length, diameter, *etc*., an extensive summary is provided, describing several techniques to perform experimental analysis and giving plausible reasons for attributing these changes. Consequently, we explore the specific areas of applications for these CNT-reinforced composites in fields such as aerospace, energy, biomedical, and automobile, and how they can be further processed and changed to allow for more affordable and efficient solutions in the future.

Keywords: carbon nanotubes, materials processing, experimental analysis, challenges, applications, composites, microscopy

*** Corresponding author: S. Aravind Raj,** Department of Manufacturing Engineering, School of Mechanical Engineering, Vellore Institute of Technology, Katpadi, Vellore – 632014, Tamil Nadu, India, e-mail: aravindsakthivel@hotmail.com
*** Corresponding author: Mohamed Thariq Hameed Sultan,** Department of Aerospace Engineering, Faculty of Engineering, Universiti Putra Malaysia, 43400 UPM Serdang, Selangor, Malaysia; Laboratory of Biocomposite Technology, Institute of Tropical Forestry and Forest Products (INTROP), Universiti Putra Malaysia, 43400 UPM Serdang, Selangor, Malaysia; Aerospace Malaysia Innovation Centre (944751-A), Prime Minister's Department, MIGHT Partnership Hub, Jalan Impact, 63000 Cyberjaya, Selangor Darul Ehsan, Malaysia, e-mail: thariq@upm.edu.my
Megha Choudhary: Department of Electrical and Electronics Engineering, School of Electrical Engineering, Vellore Institute of Technology, Katpadi, Vellore – 632014, Tamil Nadu, India
Aaruni Sharma: Department of Manufacturing Engineering, School of Mechanical Engineering, Vellore Institute of Technology, Katpadi, Vellore – 632014, Tamil Nadu, India
David Hui: Department of Mechanical Engineering, University of New Orleans, Louisiana, United States of America
Ain Umaira Md Shah: Department of Aerospace Engineering, Faculty of Engineering, Universiti Putra Malaysia, 43400 UPM Serdang, Serdang, Malaysia

1 Introduction

Carbon-based research started gaining traction between 1970 and 1980, during which period it was discovered that the decomposition of hydrocarbons produced carbon filaments with very small diameter, at high temperatures in the presence of catalyst particles [1]. A breakthrough occurred with the discovery of fullerene in 1985, when graphite was vaporized by laser irradiation leading to the formation of C60 atoms [2]. Following the discovery of carbon nanotubes (CNTs) in 1991, [3] there have been tremendous advancements in the domain of carbon-based research, finding applications in various fields such as electronics, healthcare, additive manufacturing, and more.

CNTs are a kind of tubular structure typically having a diameter in nanometer and length in micrometer [4]. They can be categorized into three types, single-walled CNTs (SWCNTs), double walled CNTs (DWCNTs), and multi-walled CNTs (MWCNTs) [5]. Their properties, such as extremely high surface areas and large aspect ratios, provide them with extraordinary mechanical strength (100 times greater than steel) and thermal and electrical conductivity similar to that of copper. The chirality of these structures also has a profound impact on the electronic properties of CNTs [6]. Various ways to synthesize these structures include the carbon-arc discharge method, laser ablation carbon, and chemical vapor deposition (CVD) [7,8], which will be explored in detail in this review.

CNTs have a wide variety of applications spanning various fields such as materials science, energy, electronics, sensors, and more. The excellent mechanical properties possessed by CNTs are used extensively in carbon composites and composites having CNTs as fillers. In contrast, the thermal properties can be utilized for heat dissipation, among other applications. A high surface-to-volume ratio enables CNTs to be used as sensors, especially for biomedical applications. CNTs are used in electronics as supercapacitors and actuators due to their high electrical conductivity. Apart from these, CNTs are also used as scanning probe tips for hydrogen storage, nanoelectromechanical devices, and more [9–11]. The biomedical applications of CNTs range from tissue engineering, promoting neuronal outgrowth, to developing robust and lightweight prosthetics and neuro-prosthetics because of their ability to interact with electrically active tissues and outstanding flexibility [12,13].

However, CNTs come with their fair share of challenges that need further research to be resolved [14]. Due to their tendency to stick together in a matrix, it is difficult to align the tubes with the matrix. CNTs need to be manufactured with longer lengths and in larger quantities economically with efficient distribution in the matrix.

With the rapidly advancing industrialization, there is an urgent need for material composites that can resolve the issues mentioned above and are light, have excellent mechanical and thermal properties, and have a varied field of applications. Graphene is a possible substitute for CNTs in composites but lacks the superior mechanical strength of the latter [15]. Over the past decades, there has been an exponential growth in the development of CNT Metal Matrix Composites (CNT-MMCs), which allow us to benefit from the properties of CNTs, such as their high tensile strength and thermal and electrical conductivity. With this review, we hope to provide a comprehensive overview of CNTs, the numerous material processing methods, their manufacturing methods, different kinds of experimental analysis and their impact on the use of CNTs in today's world. Figure 1(a) and (b) show the structure of SWCNTs and MWCNTs [13].

2 Materials processing

2.1 MMCs

2.1.1 CVD and infiltration

This popular process comprises forming a thin film on the surface of a heated substrate when treated with gaseous vapors in a vacuum. It can be used to fabricate CNT/Al composite foams. Using a C_2H_2/Ar mixture flow, CNTs can be manufactured using Co/Al as the catalyst at 600°C. An Ar atmosphere can cool down the system to finally produce CNT/Al composite powders [16,17].

In a similar process, chemical vapor infiltration can be utilized to form composites by diffusing reactant gases into a heated fibrous preform, followed by the reaction to a solid phase on the fiber's surface. CNT/SiC composites can be formed using this, where methyl trichlorosilane acts as a precursor gas, hydrogen as a carrier gas, and argon as diluting gas, and the CNT is placed into the chemical vapor infiltration furnace for infiltration [18].

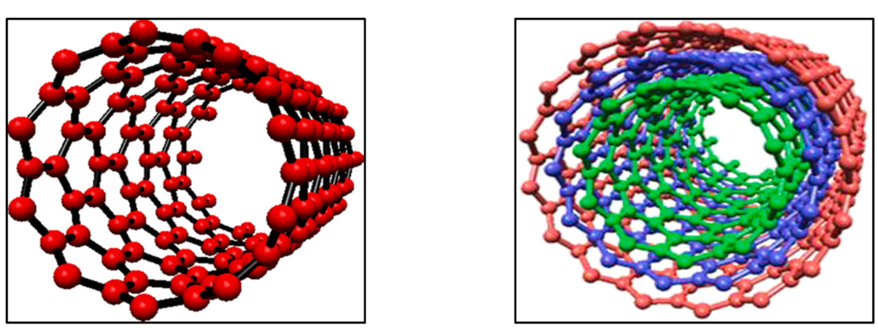

(a) (b)

Figure 1: (a) Structure of SWCNT and (b) structure of MWCNT.

2.1.2 Spray pyrolysis

Another method to form CNT-metal composites is spray pyrolysis, where a fine film is deposited on a heated surface by spraying or injecting the precursor on the heated surface. This method can be used to prepare the precursor CNT–Cu_2O. Initially, Cu powders and CNT dispersions are dissolved in deionized water and magnetically stirred, and the resultant solution is broken down in an ultrasonic nebulizer, and the droplets are deposited in a heated reactor where solvent evaporation, solute precipitation, precursor decomposition, and sintering are carried out to give rise to the composite powder [19].

2.1.3 Ball milling

One of the most common methods of fabricating CNT-metal composites is ball milling which consists of grinding the mixture in a hollow, rotating cylindrical chamber into an excellent powder. It is usually carried out in combination with other processes such as CVD, spray pyrolysis, and cold pressing [20–22].

2.1.4 Mechanical alloying

The mechanical alloying process is a dry, high-energy ball milling method that involves recurring cold welding, followed by fracturing and then welding the blended powder again to create a homogenous composite. One of the ways this can be done, taking the case of Al6061 powders as an example, is by alloying zirconia balls, Al6061 powder, and CNTs by placing them in a zirconia jar and mixing them at speeds as high as 1,200 rpm. Following this, alcohol is added, and the mixture is ultrasonicated for 60 min. Numerous drops of the solution were taken separately and diluted until the CNTs dispersed. The processed material was then placed on an aluminum foil and pressurized at 50 MPa for half an hour to amalgamate the composite [23]. The exact process can also be done in a tungsten carbide jar using Toluene as a process control agent, rotating at 250 rpm for 6 h. The amalgamation can be done by spark plasma sintering (SPS) at a pressure of 50 MPa at a temperature of 550°C [24].

2.1.5 Powder metallurgy

Fine powders are blended and pressed into the required shape and heated just below their melting points. This technique can synthesize CNT-Al composites; Al powder, fly ash, and MWCNTs can be milled with stainless steel balls for 2 h at 250 rpm using methanol as a control agent. The resultant product can then be cold compacted at 280 MPa and sintered for an hour in an Argon environment for 500°C [25,26]. Alternatively, the milled mixture can also be hot-pressed in a vacuum at 50 MPa for 30 min at 580°C [27]. SPS can also consolidate the milled sample at 550°C at a pressure of 30 MPa. After preheating at 500°C for 3 min in an Argon environment, hot extrusion can be performed using a 2,000 kN hydraulic press [28].

2.1.6 Electrophoretic deposition

This technique makes use of the process of electrophoresis to disperse and cumulate electrolyte particles toward the anode surface in the presence of a high electric field to form a coating. CNTs can be incorporated in TiO_2 films (with ultrasonically purified titanium foil acting as the substrate) using a voltage of 350 V for 40 s, keeping the electrolyte at 20°C [29].

2.1.7 Stir casting process

Stir casting involves mechanical stirring to mix reinforcement in the material matrix. This process is based on the Taguchi method, and it is used to form aluminum alloy and CNT composites. The stir casting process results in an increase in the hardness values compared to the normal casting method and a decrease in the porosity of the cast metal [30].

2.1.8 Friction stir processing (FSP)

Based on the friction stir welding principle, this method modifies the properties of the metal through severe deformation. CNT/Al composites can be formed by combining the processes of powder metallurgy and FSP. CNT/Mg composites can also be produced using this process which considerably reinforces the microhardness of the product. Other compounds such as polyethylene, $AlSi_{10}Mg$, and Al–Mg alloy can also be reinforced with CNTs using FSP [16,31].

2.1.9 Colloidal mixing

This blending method develops hot uniaxially mixed composites with CNT addition. This process can be used to make CNT-Nickel MMCs with required fractions of CNT.

The process includes dispersion of CNT mixed with metallic powder in an ultrasound bath which is then evaporated to get the desired product [32].

2.1.10 Equal-channel angular extrusion

This process aids in the production of ultra-fine refined materials and is extensively used for Al composites. A die with a 20 mm diameter is used with the outer corner angle as 20° and channel angle as 120° on the route B_c with a ram speed of 0.8 mm s^{-1} [33].

2.1.11 Molecular level mixing (MLM)

This method constitutes mixing CNTs and the metal matrix uniformly in an aqueous solution at a molecular level. Cu composites can be manufactured using this, when MLM is performed with microwave sintering and rolling technology. To enhance the composite structure further, sintered CNT/Cu composites can be cold rolled up to 70% and annealed at 600°C for 2 h [34]. Another option can be to disperse CNTs in deionized water to get an ink-like solution, and copper acetate monohydrate can be dissolved in water, followed by magnetic stirring for 30 min. The two solutions can be mixed and heated up to 75°C for 5 min, and NaOH and 2 M glucose can then be added. After the color turns brick red, stirring has to be stopped, and the final composite can be attained by filtering and vacuum drying [35].

2.2 Polymers, ceramics, and composites

2.2.1 Pickering emulsion method

This method involves extracting cellulose nanocrystals from micro-fibrillated cellulose using acid hydrolysis followed by the addition of CNTs to the CNC suspension. The obtained suspension is ultrasonicated, and polylactic acid (PLA) is added for preparing the Pickering emulsion, which is used to prepare the PLA/CNT/CNC composites by compression molding [36].

2.2.2 Polymer infiltration

In this process, CNT films developed using CVD are immersed in polyvinyl alcohol solution and nitric acid followed by extraction of CNT fibers by shrinking the CNT film [37].

2.2.3 Hot pressing

Hot pressing is a densification process for forming powders by applying heat and pressure simultaneously in a simple die. This process is performed at temperatures high enough to enable creep processes and sintering. CNT-reinforced WC-Al_2O_3 cemented carbides can be produced using this technique [38].

2.2.4 Hot isostatic pressing (HIP)

This process involves densifying materials under very high temperature and pressure in a gas medium. For processing CNT/Si_3N_4 composites, a two-step sinter-HIP process can be used with high purity nitrogen as the pressure medium [39].

2.2.5 Vacuum bag oven process

This process involves using a flexible bag and vacuum to assist in holding layers together while the curing process takes place. CNT nanocomposites can be created using this process to ensure uniformity in the process [40].

2.2.6 Layer by layer (LBL) drafting

LBL drafting is used to prepare homogeneously distributed CNTs effectively. The process involves depositing two interactive materials onto the surface of the substrate alternatively. LBL drafting can be used for any shape or size and has the distinct advantage of being an easy to control process without any need for specialized tools [41].

2.2.7 SPS

This sintering method involves passing pulsed direct current in electrically conducting die under uniaxial pressure. SPS enables the densification of materials at comparatively lower temperatures and shorter holding times. B_4C composites can be densified using this process using graphite punch rods and die [42].

2.3 Additive manufacturing

2.3.1 Fused deposition modeling (FDM)

CNTs can be combined with polymers such as PLA, thermoplastic polyurethane (TPU), and others to obtain reinforced filaments for FDM. This process can be used to three-dimensional (3D) print CNT-yarn-based components [43], CNT-graphene-based conductive polymer nanocomposites [44], functionalized nanocomposite filaments to produce multiaxial force sensors [45], and CNTs/PLA composites [46]. Polybutylene terephthalate powder is mixed with CNT and graphene and then extruded to obtain the filament in one such process. The FDM process can also produce CNT-enabled electrodes for Li-ion batteries, which have enhanced ion and electron transport capabilities [47].

2.3.2 Selective laser melting (SLM)

SLM uses a power source in the form of a laser to melt and fuse the metal powder to obtain the product, as shown in Figure 2. SLM can be used effectively for additive manufacturing of metals reinforced with CNTs. In one such process, NiCrAlY-CNT powder is processed *via* SLM for producing substrates that are further coated with lanthanum zirconate using plasma sprayed coating deposition. Figure 2 demonstrates the process of SLM [48]. Metallic components like CNT-decorated titanium alloy powders are also manufactured using laser powder bed fusion processes [49].

2.3.3 Selective laser sintering (SLS)

Figure 3 shows the SLS process which involves a laser power source to sinter the material in powder form to create the final product. This technique can be used to create products with complex geometry easily, as shown in Figure 3. CNT-reinforced composites such as CNT/alumina composites and high-performance polymers like polyether ether ketone (PEEK) can be produced *via* SLS process [50–52].

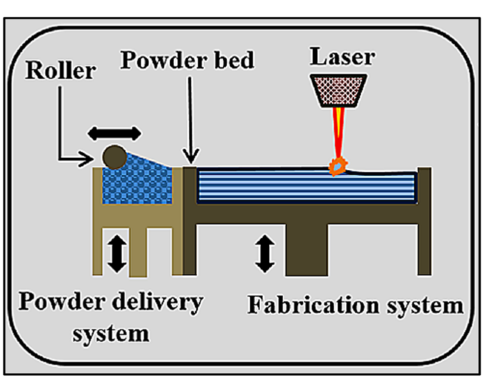

Figure 2: Selective laser melting process.

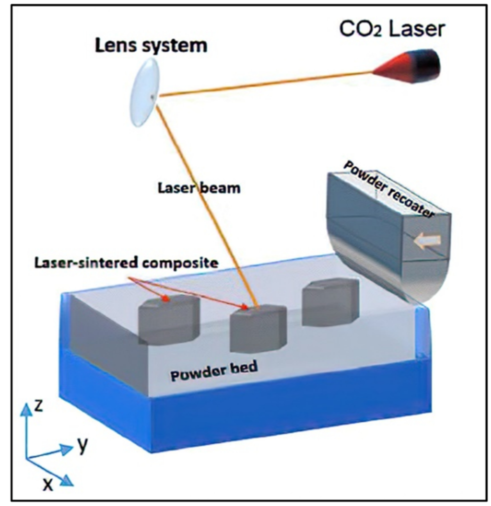

Figure 3: Selective laser sintering process.

2.3.4 Digital light processing (DLP)

This additive manufacturing process is based on curing a photopolymer resin using a directed light source to obtain the product. DLP enables 3D printing of photocurable formulations consisting of CNTs to develop composites with improved electrical properties [53].

2.3.5 Direct write printing

In this process, a viscoelastic liquid is used as the 3D ink for the manufacturing process without requiring a heat or light source. Epoxy nanoclay CNT composites can be created by sonicating the dispersion of CNTs in acetone along with the addition of curing agents and nanoclay, resulting in the production of ink that can be used in direct write printing [54].

2.4 Disadvantages concerning the preparation methods of CNT composites

Mechanical processing methods can induce a high propensity for reactions that take place simultaneously with other processes at the mesoscopic and macroscopic scales, such as structural disordering and mixing [55]. The dry ball milling method poses various disadvantages such as high non-uniformity in reaction and the size distribution along with noise, the additional material loss of powders, and additional impurities from the grinding media and the grinding jar in final products [56]. Spray pyrolysis is difficult to control and has a fairly poor homogeneity of the film thickness distribution over the substrate's area [57]. Powder metallurgy has its own set of drawbacks – the composite parts have low strength and ductility and there is a high cost associated with powder materials and the equipment used [58]. Stir casting also has some weaknesses: (a) a homogeneous distribution of reinforcements is requisite for achieving a high-strengthening effect, but a uniform distribution is relatively hard to obtain in stir casting; (b) reinforcing particles may be segregated by the surfacing of settling of the reinforcement in melting and casting process; and (c) gases and unwanted inclusions may be entrapped during stir casting [59]. SLS can include cool time up to 12 h, which means longer production time. It also causes low mechanical characteristics in the samples and comes with the possibility of distortion of geometry in case of non-observance of technological procedures for impregnation with wax [60]. In SLM, it is difficult to obtain single-phase material with the annealing step and quenching after annealing causes internal strains [61]. For SPS, only simple symmetrical shapes may be prepared and expensive pulsed DC generators are required [62].

3 Challenges in the fabrication of composites

CNT reinforcement provides numerous benefits, in terms of increasing the mechanical strength, thermal conductivity, or electrical conductivity. However, the process is not easy as it comes with its own set of challenges which have been outlined below:

(i) *Chemical functionalization may warp the bonding of graphene sheets*

The presence of functionalities such as carbonyl, carboxyl, and hydroxyl groups increase the interface strength between CNTs and the polymer matrices. Moreover, they also cause the CNTs to be dispersed more effectively. Nevertheless, chemical functionalization can reduce the mechanical properties in the CNT composite as they disrupt the bonding of graphene sheets [63].

(ii) *Size difference between CNT and matrix powders*

When CNTs larger than 1% in weight are used, they impede the achievement of required properties. The clusters present in such composites lead to reduced ductility, strength, and stiffness. Effective dispersion of CNTs can be done by milling, but those conditions lead to severe strain hardening of the matrix powders, making it difficult to process the composite further by conventional powder metallurgy [64].

(iii) *Ineffective dispersion of CNT in the matrix due to van der Waals forces*

Due to strong van der Waals forces, a large specific surface area, and a high aspect ratio, CNTs tend to agglomerate, entangle, and form clusters [65]. This phenomenon is highly undesirable as it prevents effective homogeneous dispersion of CNTs and can act as defects. This agglomeration leads to poor solubility [66], poor adhesion [50,67], and a considerable increase in the porosity and viscosity of the composite [68]. Inhomogeneous distribution might adversely affect the thermal and electrical properties due to interconnections among CNTs in the 3D networks. There have been proposals to use simple ultrasonic dispersion to overcome the strong van der Waals force [69], but this might create more significant problems. The high-energy ball milling can ruin the structure of CNTs, and the irreversible formation of metal oxides will weaken the beneficial mechanical properties of the composite [23]. Densification, which has to be performed at high temperatures in CNT/ceramic composites, might also cause CNT degradation [35,70].

(iv) *Improper bonding at CNT–matrix interface*

The proper bonding at the CNT–matrix interface plays a significant role in effective load transfer between phases [21,71]. However, the wettability of metal alloys poses a considerable problem and lowers the mechanical strength of the composite [68,69]. It can cause the CNTs to pull out from the metal matrix or fracture the CNT–metal interface [71].

(v) *Delamination of composites*

Carbon-fiber-reinforced PEEK (CF/PEEK) is thermally stable, has high chemical resistance, and thermal stability and is widely used in aviation [72]. However, delamination, *i.e.*, the material fracture, can significantly qualify these composites' applications. The poor interfacial strength between the fiber reinforcements and the polymeric matrix is caused by the homophobic and chemically inert nature of CF and PEEK. The introduction of oxygen-containing functional groups improves the shear strength of these composites but at the expense of their tensile strength.

4 Experimental analysis

Tables 11–14 give a detailed overview of the effect of fabricating CNT-composites on their mechanical, thermal, electrical, and tribological properties by studying their methods of preparation, testing methods, the properties affected and changed, and the possible reasons for their change.

4.1 Mechanical properties

Table 1 shows the comparative analysis of the mechanical properties of CNT composites.

4.2 Thermal properties

Table 2 shows the comparative analysis of thermal properties of CNT composites.

4.3 Electrical properties

Table 3 displays the comparative analysis of the electrical properties of CNT composites.

4.4 Tribological properties

Table 4 displays the comparative analysis of the tribological properties of CNT composites.

4.5 Raman and XRD spectrum analysis

Table 5 shows the Raman and XRD spectrum analysis.

4.6 Modeling of CNT composites to theorize change in the parameters

4.6.1 Modeling based on CNT waviness

On analyzing wavy CNTs using 3D representative volume element using pullout technique, it was found that the interfacial shear stress of wavy CNTs is higher than straight ones and increases with the increase in waviness [127]. For CNT/shape memory polymer composites analyzed using analytical micromechanical methods, predicted effective mechanical properties were found to be significantly decreased [128]. In the case of carbon nanotube reinforced polymer (CNRP) on the basis of multiscale modeling, wavy CNTs result in Young's modulus reduced by 25 to 50%, while the Poisson's ratio for wavy CNTs was found out to be slightly higher than that of straight CNTs [129]. When analyzed using simplified unit cell methods, CNT-reinforced polymer hybrid nanocomposites demonstrate that the wavy CNT nanocomposites have higher thermal conductivity than straight CNT ones. A multistage micromechanical analysis indicates that it enhanced the transverse thermal conductivity of hybrid nanocomposites with straight CNTs and increased in CNT length and volume fraction [130]. Another micromechanical method estimates that thermal conductivity increases nonlinearly with increasing CNT volume fraction [131].

4.6.2 Modeling based on other properties of CNTs

Molecular dynamic simulations for CNT-reinforced metallic glass nanocomposites conclude that adding CNTs result in significant changes in the lateral and axial mechanical properties. The use of long CNTs leads to an increase in the strength and stiffness of metallic glass and changes the mechanism for elastic and plastic deformation [132]. Another molecular dynamic simulation for CNT reinforced aluminum composites shows that toughness, Young's modulus, and other mechanical properties are enhanced significantly with an increase in CNT reinforcement, thus enabling the material to support extra loading and prevent fracture in the metal matrix [133]. Shear lag and Schapery models for determining the stiffness of CNT-reinforced metal matrix nanocomposites show that the addition of CNTs leads to an increase in stiffness and initial yield surface size. Decreasing the CNT diameter, while increasing the volume fraction and length results in improved transverse elastic modulus and size of the initial yield surface [134]. Estimation of effective elastic properties of CNT/polymer composites demonstrates remarkable enhancement in elastic moduli due to changes in matrix and filler interface of polymer composites [135]. A unified model developed for free vibration analysis of CNT-reinforced laminated cylindrical shells shows that the addition of CNTs improves the natural frequency of the shell, registering a maximum increase of 50% in frequency [136].

5 Applications of CNT-reinforced composites

CNTs, with their lightweight structure, thermal, electrical, and mechanical properties, find use in a variety of applications. We have outlined below the different

Table 1: Comparative analysis of mechanical properties of CNT composites

Sl. no.	Matrix	Method of preparation	Testing method	Property affected	Change observed	Possible reason for change
1	Alumina [73]	(i) Tape casting, lamination, and hot pressing	Ball-on-reciprocating wear tester under an unlubricated condition at room temperature	Weight loss	(i) 12% decrease	Grain size effect and reinforcement effect of CNT
		(ii) Hot pressing			(ii) 4% decrease (increases after further CNT addition)	
2	Polymer (PET, polypropylene (PP), and PE) [74]	Catalytic decomposition of propylene on Fe/Al_2O_3 catalyst followed by compounding the polymer using a twin-screw extruder	Scanning electron microscopy (SEM) and high-resolution transmission electron microscopy (TEM)	(i) (a) Loss factor of composites (b) reflectivity peak moves (ii) Absorbing peak changes	(i) (a) Increases (b) moves to a lower frequency (ii) Peaks occur at 7.6 and 15.3 GHz	Dielectric loss is much higher than that of magnetic loss especially in frequencies ranging from 6 to 18 GHz
3	Cu [75]	Molecular level Process	Scanning electron microscopy. high-resolution TEM, Vickers hardness test, and pin-on-disk type wear tests	Hardness changes	Linear increase up to 1.1 GPa	The strength of the bond at the CNT/Cu interface, the homogeneous distribution of CNTs within Cu matrix, and attained high relative densities.are possible reasons for the mentioned change.
4	Ni–P–CNT coated copper composite [76]	Electroless composite plating process	X-ray spectrometer	Young's modulus and tensile strength affected	(i) Increase if CNT is non-activated (ii) Decrease if CNT is activated	Different processing methods of CNTs before electroless composite plating can lead to totally different effects on the mechanical properties of Ni–P–CNTs coated copper composite materials
5	Aluminum [64]	Ball milling, cold compaction, and hot extrusion	Field emission scanning electron microscope (FE-SEM) and TEM	(i) Young's modulus affected (ii) Tensile strength affected	(i) 50% strength increased after adding 2 wt% CNT; no increase observed on further CNT addition (ii) 23% strength increased after adding 2 wt% CNT, drops slightly at 5 wt%	The better dispersion of CNTs provided by ball milling in addition to the strain-hardened powders contributes as a strengthening mechanism to the final strength of the composites
6	Diamond-like carbon (DLC) films [77]	Dispersion, spin coating, and DLC deposition	Nanoindentation	(i) Elastic modulus and hardness affected (ii) Friction coefficient affected	(i) Increases with CNT doping (ii) Decreases with the increase in the CNT doping	Anisotropic property and the orientation effect of CNT

(*Continued*)

Table 1: *Continued*

Sl. no.	Matrix	Method of preparation	Testing method	Property affected	Change observed	Possible reason for change
7	CNT-reinforced basalt/epoxy composites [78]	Impregnation of woven basalt fibers into epoxy resin mixed with CNTs	Dynamic mechanical analysis	Young's modulus and tensile strength affected	60 and 34% increase, respectively, compared to unmodified composite	Improved dispersibility and strong interfacial interaction between the silane functionalized CNTs and the epoxy in the basalt fabric/epoxy composites
8	Magnesium alloy ZK60A [79]	Disintegrated melt deposition technique and hot extrusion		(i) 0.2% tensile yield strength (YS) and ultimate tensile strength (UTS) affected (ii) 0.2% compressive YS and ultimate compressive strength affected (iii) Microhardness affected	(i) 10% increase observed (ii) −14% and +5%, respectively (iii) 17% decrease observed	(i) Overall positive effect derived from lower grain size and well-known factors of reinforcement (ii) Overall negative effect derived from (a) significantly reduced precipitation of intermetallic phase(s) in the nanocomposite matrix compared to monolithic material and (b) compressive shear buckling of CNT in the nanocomposite.
9	Carbon fiber/epoxy composite [67]	Fabricated by incorporating woven-type carbon fibers into epoxy matrices modified with 2 wt% acid-treated and silane-treated MWCNTs	Three-point bending and ball-on-disk wear tests	(i) Flexural moduli and strengths affected (ii) Wear properties changed	(i) 34 and 20% greater, respectively, than those of the acid-treated carbon/CNT/epoxy composites (ii) Alson improved	Improved dispersibility and interfacial interaction between the silane-modified MWCNTs and the epoxy in the carbon/epoxy composites.
10	Ni/CNTs hybridization on CNTs/epoxy nanocomposites [80]	CVD and electroless Nickel plating	SEM, X-ray spectroscopy, and inductively coupled plasma mass spectrometry	Shear viscosity changes	Small amount (0.8 wt%) of Ni/MWCNTs induced a slight increase in the viscosity	Good dispersion behaviors of the Ni-coated MWCNTs in the matrix
11	Epoxy/CNT [81]	Magnetically stirred, ultrasonically treated, sprayed, and curated	SEM and TEM	Critical stress intensity factor (K_{IC}) changes	A 38% increase in K_{IC} was observed when compared to neat epoxy resins	Functionalization of CNTs significantly increased the fracture properties of the DGEBA/CNT composites, which was attributed to the improved dispersion of CNTs in an epoxy matrix and interfacial interactions between the functional groups on the CNT surfaces and the epoxy matrix

(*Continued*)

Table 1: *Continued*

Sl. no.	Matrix	Method of preparation	Testing method	Property affected	Change observed	Possible reason for change
12	CNT/Al–Cu composites [82]	MLM and a high energy ball milling process	Artificial aging heat treatment	YS and UTS changes	YS increases from 110 to 384 MPa, while the UTS doubles	Homogeneous dispersion of CNTs in Al–Cu matrix and the fracture surface of CNT/Al–Cu composites
13	CNT/2009Al composites [65]	Powder metallurgy (PM) followed by 4-pass FSP	Elevated temperature tension and coefficient of thermal expansion (CTE) measurements	YS affected	(i) At 293–573 K, enhanced compared with that of the 2009Al alloy (ii) Exhibited significantly increased YS compared to the 2009Al alloy and 1.5 vol% CNT/2009Al composite, and decreases on further temperature increase	(i) Resulted from load transfer mechanism (ii) The dimples became shallow, and when the temperature reached 573 K, the composites showed an obvious intergranular fracture
14	CNTs-reinforced Sn–58Bi composites [83]	Ball milling in an argon atmosphere	Three-point bending tests and SEM	Bending strength and toughness change with respect to Sn–58Bi alloy	10.5 and 48.9% increase observed, respectively.	Bending strength increases because of the refinement of the Bi-rich phase. Also, during the fracture process, CNTs were pulled out from the matrix alloy leading to the formation of pseudo-dimple, which can elongate the micro-crack and increase the fracture area dramatically
15	Ni–P–CNT composite [84]	CVD, ball milling, and electroless deposition	SEM, atomic force microscopy (AFM), X-ray diffraction (XRD), energy dispersive spectroscopy (EDS), and Vickers measurements	Microhardness values of coating changed	Significantly increases	Precipitation hardening effect generated by the precipitation of the Ni_3P phase in the nickel matrix
16	CNT-reinforced porous CuSn oil bearings [85]	Powder metallurgy method	TEM, SEM, and digital light optical microscopy	Microhardness and radical crushing strength affected	Steadily improve with the increase in the content of CNTs from 0 to 2.0 wt%; decline when the content of CNTs is higher than 1.0 wt%	Increase caused by even dispersion of CNTs; too much CNT will degrade pore structure
17	Reactive oligomers and epoxy–MWCNT composite [86]	Dried poly(ethylene oxide) (PEO) was added to isophorone diisocyanate for 30 min in a N_2 atmosphere,		(i) Impact strength at room temperature and cryogenic temperature affected	(i) Increased by 23.6 and 69.5%, respectively, compared to the unmodified epoxy	The presence of the oligomer in the modified epoxy facilitates the dispersion and interfacial interaction of the O-CNTs with the

(*Continued*)

Table 1: *Continued*

Sl. no.	Matrix	Method of preparation	Testing method	Property affected	Change observed	Possible reason for change
		followed by defluxion for 2 h at 80°C. The reactive oligomer, after mixing with dried epoxy, was stirred at 80°C for 4 h		(ii) Tensile strength mostly unaffected		epoxy, which improves the toughness of the epoxies
18	B_4C/CNT composites with Al additive [87]	Fabricated by hot pressing using Al additive	SEM, Vickers hardness test, and X-ray diffractometry	(i) Vickers hardness (ii) Elastic modulus	(i) Almost constant, decreases with increase in CNT after 5 vol% CNT (ii) For 0.5 vol% CNT, comparable to the value of B_4C; for more than 2 vol% CNT, decreases with a linear increase in CNT content	(i) This can be explained by the presence of higher CNT quantities at grain boundaries (ii) Due to the effects of mismatched interfaces between B_4C and CNT and the orientation of the CNTs
19	CNTs/Mg–6Zn composites [88]	Fabricated by CVD with different solidification rates of the composites	SEM and TEM	YS and UTS affected	YS and UTS increase by 18 and 13% for lower solidification rate composite. For a higher solidification composite rate, YS and UTS increase by 50 and 36%, respectively	Good dispersion of CNTs in the Mg metal matrix and good interfacial bonding between CNTs and matrix. Also, CNTs can act as solidification nuclei and restrict grain growth by the pinning effect during solidification
20	CNT/Al composite [89]	Ball milling	SEM and TEM	Tensile elongation	(i) Increases by 1.4–2.5 times (ii) Decreases when compared to milled pure Al	The strain rate sensitivity intensifies at high strain rates
21	CNTs/Mg–6Zn composite [90]	Hot extrusion	SEM, TEM, and electron backscatter diffraction analysis	YS, UTS, modulus, and elongation	(i) 10, 8, 7.5 and 22% increase observed, respectively (ii) 33, 18, 30, and −22% increase observed, respectively (iii) 25.4, 13, 56, and −54% increase observed, respectively	The grain refinement effect, load transfer mechanism, and Orowan mechanism of CNTs
22	Graphene nanoplatelets (GNPs) and CNTs [91]	Semi-powder metallurgy method with vacuum sintering technique followed by hot extrusion	XRD, SEM, and TEM	Elastic modulus, 0.2% YS, UTS, and failure strain	+17%; +19%; +15% and +137% increase, respectively	Dislocation generation due to mismatch in CTE and elastic modulus between matrix and reinforcement. Efficient load

(*Continued*)

Table 1: *Continued*

Sl. no.	Matrix	Method of preparation	Testing method	Property affected	Change observed	Possible reason for change
						transfer and absence of intermetallic phase also significantly contribute to basic strengthening mechanism
23	CNT/epoxy composites [92]	Drawing, winding, and pressing	FE-SEM and Raman spectroscopy	Tensile strength and elastic modulus	12 and 14% increase in CNTs with a diameter of 22 nm when compared to CNTs with a diameter of 38 nm	Larger diameter CNTs show a lower effective modulus and occupy a more significant volume fraction in the composite than smaller diameter CNTs do; minimal load transfer due to weak Van der Waal's interaction
24	CNT/epoxy composites[93]	CNTs, intermixture of epoxy resin, and the corresponding diamine-based hardener were dissolved in a large portion of solvent phase	Nano indentation	Young's modulus	Almost identical for 20% CNT content, an increase by 330% for CNT content of 60%, decreases on further increasing CNT content	Air inclusions caused by an insufficient molding pressure during composite processing
25	CNT-filled glass fiber/epoxy composite [94]	MWCNT was first dispersed in 150 mL acetone which was then stirred at 1,000 rpm for 1 h followed by 1 h of bath sonication. After adding preweighed epoxy, the suspension was stirred at 70°C at 1,000 rpm till all the acetone evaporated. Sonication was then performed at 70°C for 1 h	Short beam shear (SBS) test and flexural test	Modulus and strength affected	11.5 and 32.8% increase, respectively, when tested at room temperature; gradually decreases when CNT content exceeds 0.1%	Efficient stress transfer from the soft polymer matrix to the stiff MWCNT through the subtle CNT/polymer interface
26	Glass- and carbon-fiber-reinforced plastic (GFRP and CFRP) composites with CNT fibers [95]	Vacuum infusion		Average tensile strength changes	6.9% higher strength in GFRP than those without CNT fibers and a 2.5% increase in CFRP	The load carried by the CNT fibers and the epoxy resin coating layer applied to the surface of the specimens to fix the position of the CNT fibers
27	CNT-Cu composites [96]			Young's modulus, yielding strains, tensile strength, and compressive strength	Young's modulus increases by 32%, yielding strain decreases, tensile and compressive strength increase by 14 and 66%, respectively	The inclusion of CNT into the Cu, matrix precipitates the formation of dislocations and slip planes in a different way, depending on the loading nature

(*Continued*)

Table 1: *Continued*

Sl. no.	Matrix	Method of preparation	Testing method	Property affected	Change observed	Possible reason for change
28	TiC-modified CNT-reinforced Al [97]	Ultrasonication, wet milling, and tip sonication	Raman spectroscopy, XRD, TEM, SEM, and nanoindentation	Vickers hardness, nano hardness, and Young's modulus affected	176, 82, and 48% increase observed when compared to pure Al sample	A combination of abrasive and oxidation wear contribute to the mechanisms of the samples
29	Functionalized carbon nanotubes (FCNTs) with fiberglass/epoxy laminates [98]	Synthesized CNTs were oxidized by refluxing at 130°C in an acid mixture for 30 min, diluted with water and filtered. The filtered samples were washed by distilled water and dried in an oven at 50°C for overnight, thus obtaining the FCNTs	SEM	Tensile strength and elasticity modulus (*E*)	Increased by ~7 and 6%, respectively, correlated with the original sample. On adding CNT up to 0.35 wt%, increases by 30 and 31%, respectively; decreases on further addition	Mixing of FCNTs with epoxy restricted the molecular rearrangement of epoxy chains during the mixing, preparation, and solidification processes
30	CNTs with concrete [99]	Sonification, dispersion, mixing, compacting, and demolding	SEM	Compressive, flexural, and tensile strength	23, 29, and 20% increase, respectively	
31	CNT-(Mg-6Zn) [100]	CVD, semisolid stirring assisted with ultrasonic vibration method	SEM and optical microscopy	E, YTS, UTS, elongation and residual stress affected	increased by 9.6, 14, 20, 18.2%, respectively, while residual stress drops from 74 to 35 MPa	CNTs-(Mg-6Zn) interface layer is formed, which allows the grain refinement and the low residual stress, which contributes to enhancing the mechanical properties of composites
32	CNT and GNPs reinforced PEEK composites [52]	Stir mixed prior to melt compounding	SEM and Vickers hardness test	Young's and storage moduli affected	(i) Increase by 20 and 66% (ii) Increase by 23 and 72%	Influenced by factors such as the bead–bead interfacial strength, nanostructure–PEEK interfacial strength, the dispersion state of the nano reinforcement, interfacial voids between beads, and the voids within the beads
33	CNTs/Cu matrix [101]	Ball milling	FE-SEM and TEM	Strength and ductility change	18 and 14.3% increase	Uniform distribution of reinforcements, good interfacial bonding, and extrusion pressure acting on CNTs due to the filling of Cu inside the tubes

Table 2: Comparative analysis of thermal properties of CNT composites

Sl. no.	Matrix	Method of preparation	Testing method	Property affected	Change observed	Possible reason for change
1	Aluminum and graphite with CNT thermal interface material [102]	(i) Tape casting, lamination, and hot pressing (ii) Hot pressing	SEM and light flash apparatus	Thermal conductivity	There was a 300% increase with graphite coating for Al samples and 350% with CNT interface. There was a 250% increase with graphite coating and 350% with CNT interface for graphite samples.	Without any interface material, air trapped in the micro-gaps created a thermal resistance bringing down the thermal conductivity. The thin CNT sheet thermal interface material helped provide a high conductivity heat transfer path, thus minimizing the effect of micro-air gaps resistance
2	CNT-reinforced basalt/ epoxy composites [78]	Impregnation of woven basalt fibers into epoxy resin mixed with CNTs	Dynamic mechanical analysis	Glass transition temperature	Gradually increases	The difference in the extent of cross-linking reactions of epoxy and the silane molecules make more covalent bonds with CNTs and a higher cross-linking network than the unmodified and oxidized samples
3	CNTs and intumescent flame retardant (IFR) embedded in PP [103]	Melt blending	Thermogravimetry (TG) and cone calorimetry tests	Thermal stability and flammability	Improvement in thermal stability compared to PP/IFR composite before the T_{max} but severe deterioration of flame retardancy	The efficient barrier effect of carbonaceous char formed by the incorporation of CNTs and IFR at relatively low temperatures and the decrease in the protective effect of intumescent char on underlying polymer materials
4	Epoxy/CNT [81]	Magnetically stirred, ultrasonically treated, sprayed, and curated	Thermogravimetric analyzer	Glass transition temperature	Increases by about 11°C compared to neat epoxy resins	Reduced mobility of the epoxy matrix around the nanotubes by the interfacial interactions
5	CNT/2009Al composites [65]	Powder metallurgy (PM) followed by 4-pass FSP	Elevated temperature tension and CTE measurements	CTE	Decreases upon increasing the volume fraction of the CNTs	A large number of interfaces between the CNTs and aluminum matrix
6	CNT/Bi_2Te_3 composites [104]	SPS	Properties measured using a ZEM-3 unit	Seebeck coefficient and thermal conductivity	Seebeck coefficient changes from −83 to −113 μV/K upon CNT addition; thermal conductivity decreases	Decreased carrier concentration and the newly formed CNT/Bi_2Te_3 interface cause a lattice phonon dissipation and hot carrier scattering
7	CNT/bismaleimide (BMI) composites [105]	CVD and spray winding	Thermal diffusivity measured with laser PIT device	Thermal conductivity changes with CNT diameter	1.1 mmlong CNTs show 112% improvement over the composites containing 0.65 mm long CNTs; no change upon further change in length and diameter	Weak tube–tube coupling, dangling tube ends, misalignment, and structural defects

(*Continued*)

Table 2: *Continued*

Sl. no.	Matrix	Method of preparation	Testing method	Property affected	Change observed	Possible reason for change
8	Calcium ferrite-CNTs/PET nanocomposite [106]	Melt compounding	Thermogravimetric (TGA) analysis	Thermal stability affected	Thermal stability shows a marked improvement	Either the barrier effect of the nanofiller dispersed into the PET matrix, respect to the volatile decomposed products, as well as the air gases permeating through the nanocomposites, or to an effect of the trap action exercised by CNTs on the polymer peroxyl radical that prevents their recombination

domains where CNT-reinforced composites have bearing depending on their diverse range of properties:

5.1 Aerospace, automobile, and military applications

CNT/polymer composites such as polyethylene terephthalate (PET), PP, and polyethylene (PE) have broad frequency ranges for absorbing values exceeding 5 dB and have potential applications as radar absorbing materials and can be extensively used in commercial and military applications [74]. Their fracture resistance and damping characteristics also make them an excellent candidate to be used in the aerospace and automotive industry [127]. CNT/Al composites with high structural strength and functional abilities are universally employed in aircraft structures [82]. When SWCNTs are added to IM7 prepreg composites, there is a considerable increase in the thermal conductivity of the composite when compared to the original material, which makes them favorable for use in the low-temperature environment of space. The efficient heat dissipation of CNTs necessary in the pipes and components of aerospace vehicles make them a good fit for rockets such as the Space Launch System [40]. A small amount of CNT can drastically increase the water resistance and interlaminar properties of CNT/epoxy composites and thus find prospective implementation in the automobile industry [137]. Likewise, CNT/SiC composites meet the requisites of advanced structural vehicles such as space vehicles due to their high strength and EMI shielding performance [138]. By combining different amounts of CNTs with nanoclay, ink can be 3D printed with enhanced mechanical and electrical properties, making them a promising composite prospect [54]. Water sustainable fly ash polymer nanocomposites are also widely used in automobile body parts due to their dielectric and water-absorbing characteristics [114].

5.2 Biomedical industry

The electromechanical sensitivity of TPU composite with ionic liquid modified CNTs is significantly high compared to dielectric elastomers, which shows application prospects in artificial muscles, prostheses, bionic robots, and wearable tactile devices [139]. The surface charge of oxidized CNT leads to improved local ionic strength during collagen fibrillogenesis and can be used in tissue engineering and for manipulating collagen's properties to direct cells' fates [140]. Muscle-based biohybrid

Table 3: Comparative analysis of electrical properties of CNT composites

Sl. no.	Matrix	Method of preparation	Testing method	Property affected	Change observed	Possible reason for change
1	CNT/polymer nanocomposites [66]	CNTs were filtered and washed with deionized water until the filtrated solution had a pH of 7. The CNTs were heated for 4 h at 292°C before the Fenton Chemistry purification in order to remove amorphous carbon impurities. The solution was then briefly sonicated (30 min) and stirred overnight. The composite solutions were cast onto glass plates that were cleaned by sequential washing with ethanol and acetone under sonication	Four probe method	Electrical conductivity	Increases with increase in CNT concentration	Dependent on various factors such as the surface functionality, tube diameter, length, wall thickness, and bundle size
2	CNT/Bi_2Te_3 composites [104]	SPS	Properties measured using a ZEM-3 unit	Electrical resistivity	Increases with CNT addition at 298 K and keeps on rising until 498 K	Due to the newly formed CNT/Bi_2Te_3 interface
3	CNT/BMI composites [105]	CVD and spray winding	Four probe method	Electrical conductivity	Increases with increase in CNT length and diameter	Longer and thicker CNTs ensure a more effective electron conduction path along the individual nanotubes, similar to the thermal conduction mechanism, and CNTs with larger diameters favor more compact structures, so the separation between CNTs decreases
4	CNT/epoxy composites [93]		Material testing machine and universal calibrator	Electrical conductivity	Increases strongly with increasing solid content, reaching a maximum value of 838 S/m at a solid content of 60 wt%, decreases again with further increased solids content	Due to the air inclusions caused by the composite processing
5	CNT/polyaniline (PANI) hybrid nanoparticles [107]	*In situ* polymerization of aniline in the presence of MWNT, with ammonium peroxidisulfate as the oxidant	DC Kelvin bridge and a standard, four-probe technique	(i) Carrier mobility	(i) Increases with increased CNT content	(i) The π-π interaction reduces the threshold for inter-chain hopping
				(ii) Electrical conductivity	(ii) Increases with increased CNT content and then plateaus	(ii) With increased doping content, MWNT/PANI particles gain proximity, at which point MWNT interconnects with the aid of a

(*Continued*)

Table 3: *Continued*

Sl. no.	Matrix	Method of preparation	Testing method	Property affected	Change observed	Possible reason for change
						conductive PANI layer. Expanded channels for transporting electrons are formed, which induces an apparent rise in carrier concentration
6	CNT and PU/PVC nanocomposites [108]	Casting technique	The nanocomposite was tested by utilizing the programmable automatic	(i) Permittivity affected (ii) Electrical conductivity	(i) Decreases with increase in frequency (ii) Increases with increased CNT content	(i) Due to direction dipoles of applied electric field (ii) Effective conductive network is formed when CNTs load in polymer blend due to the electronic and impurity contributions arising from the CNTs (percolation theory)
				(iii) Dielectric loss	(iii) Increases progressively with CNTs content	(iii) There is a higher charge carrying capacity of loaded films compared to pure blend film
7	PP as a polymer matrix and Graphite (G), Carbon Black (CB) and CNTs as reinforcements [109]	Ball milling, hot and cold pressing	Four-point probe method	Electrical conductivity	Increases initially with CNT addition from 1.0 to 6.0 wt%, decreases slightly with the CNTs filler loading concentration increased	The gaps between the synthetic graphite particles were filled effectively with CNTs, thus conducting networks were formed between the CNTs/G/CB and PP matrix. higher CNTs loading in the polymer composites may cause critical CNTs aggregation, and the electrical conductivity will be leveled off, even decreased
8	CNT/polymer matrix [110]	Probe sonication, magnetic stirring, and refluxing of CNT	Four-point probe method	Electrical conductivity	(i) Field-assisted PVDF-aligned CNT films have shown a 28% increase in conductivity in parallel direction of alignment, while transverse directions have shown a 58% decrease in electrical conductivity (ii) Alternating pulsed current passage assisted PVDF-aligned CNT film shows a 360% increase in conductivity in a parallel direction (over random sample). The transverse	Partial melting and distortion of the film due to high passage of current at 500 V during the fabrication process, which might have caused an extraordinary increase in temperature at places

(*Continued*)

Table 3: *Continued*

Sl. no.	Matrix	Method of preparation	Testing method	Property affected	Change observed	Possible reason for change
					direction becomes almost insulating	
9	GFRP and CFRP composites with CNT fibers [95]	Vacuum infusion	Two-probe method	Maximum electrical resistance change rate	Exceeded 3.15%, which corresponds to a value 10 times higher than those reported in previous studies	Both the decrease in the cross-sectional area and the formation of gaps may lead to an increase in the electrical resistance of the fiber
10	CNTs/silica composite ceramics [111]	Sonication, ball milling, vacuum-rotary evaporation	Four-probe Van der Pauw method	(i) Electrical resistivity and absorption ratio	(i) Decreased with increasing CNTs amount	(i) The formation of the electro-conductive network contributed to ensure electrons move freely in the material e
				(ii) Morphology	(ii) Denser and superior microstructure compared to composites with lower CNT content	(ii) Homogenous dispersion of carbon nanotubes in the silica matrix without affecting the formation and solidification of the ceramic bas
11	CNTs/Reduced graphene oxide (RGO) composite [112]	Freeze-drying and *in situ* catalytic grown methods.	Two probe method	Conductivity and EM absorption	Increases with CNT addition	The CNTs layer, which is around the surface of the interconnection of the RGO frame, act as the EM absorbing reinforcement
12	CNT polycarbonate composite [113]	Hot pressing and microinjection molding	Lock-in thermography	Electrical conductivity	Increased up to over 100 times after changing the melt temperature from 250 to 280° C	Due to a lower mold temperature and faster cooling in the skin region, the melt temperature decreased and increased melt viscosity and injection pressure loss resulting in a larger skin layer thickness (percolation threshold gives rise to step wise change in resistivity)
13	CNT-reinforced industrial waste fly ash based polymer nanocomposites [114]	Compressive molding and ball milling	Measured using Keysight LCR meter	(i) Dielectric constant	(i) Drastically decreases from 38 to 10 for 5% CNT filled nanocomposites	(i) Due to the conducting nature of CNT and the creation of space charge distribution in polymer matrix
				(ii) AC conductivity	(ii) Increases	(ii) Due to the formation of CNT-induced conductive network and may also be related to the percolation threshold of CNT filler
14	MWCNTs/phenolic nanocomposites [115]	Hot pressing	SEM and Raman spectroscopy	Electrical conductivity of the nanocomposite	Rapid increase by 10 orders of magnitude	Due to the formatting of the percolating network (*i.e.*, percolation threshold – between 0

(*Continued*)

Table 3: *Continued*

Sl. no.	Matrix	Method of preparation	Testing method	Property affected	Change observed	Possible reason for change
						and 0.5 wt% of MWCNT concentrations)
15	MWCNTs/glass/epoxy composite [116]	Vacuum-assisted resin infusion		Gauge factor	Increase in the percentage of MWCNTs results in the reduction in electrical resistance and strain sensitivity (Gauge factor)	Strain sensitivity of the MWCNTs-GE composites reduces due to a decrease in the distance between neighboring MWCNTs
16	GFRP and CFRP composites with CNT fibers [97]	Vacuum infusion		Gauge factor	Gauge factor is higher by 3.1	Formation of gaps and a decrease in the cross-sectional area

actuators with aligned CNT forest microelectrode arrays can be integrated into scaffolds for cell stimulation and can be used to create electric fields using low potentials to give rise to cell polarization [110]. TiC-reinforced titanium matrix composites can also be tailored for biomedical applications [49].

5.3 Electrical and electronics industry

Silver nanoparticles decorated with CNT show prospective applications in electronics packaging and assemblies, such as isotropic conductive adhesives, owing to their electrical conductivity being four times greater than pristine CNTs [141]. DLCs find use in numerous fields such as optics, microelectronics, and tooling. The addition of CNT also increases fracture toughness and reduces their internal stress, thus minimizing their limitations [77]. The evolution of electrically conducting polymers with decent air stability can bring organic materials into a degenerate semiconductor or metallic regimes and can be used to create thermoelectric materials [66]. Ni/CNTs hybridized with CNT/epoxy nanocomposites have low weight, very high strength with moderate electrostatic discharge properties, and can be used in nanoelectronic devices, flat-panel field-emission displays, and chemical sensors [80]. Polymers with carbon and metal fibers find several uses in structural reinforcement, EMI shielding, electronic packaging, radar absorption, and high-charge storage capacitors [142]. The high aspect ratio and large specific surface area of MWCNTs make them suitable for developing biosensors, thermoelectric devices, functional membranes, capacitors, and artificial muscles [50]. The conductive and highly porous nature of s-CNT-reinforced polymeric powders makes them a good fit for manufacturing electronic packaging and actuation [20]. The high performance of Li-ion batteries can also be enabled by converging nanoscale additive manufacturing [47]. CNT fibers and their derived functional materials also find fiber- or fabric-based applications such as supercapacitors, batteries, intelligent sensors, actuators, and artificial muscles [37].

5.4 Miscellaneous

Assimilating vertically aligned CNT arrays into the existing conventional structural composites makes them appropriate for erosive wear applications [119]. Ni–P-based

Table 4: Comparative analysis of tribological properties of CNT composites

Sl. no.	Matrix	Method of preparation	Testing method	Property affected	Change observed	Possible reason for change
1	Alumina–CNT composites [75]	Tape casting, lamination, and hot pressing	Ball-on-reciprocating wear tester under an unlubricated condition at room temperature	Wear rate	(i) For hot-pressed samples, it decreased with increasing up to 4 wt%, but increased with further addition of CNT (ii) For tape casted composites decreased steadily with increasing CNT addition up to 12 wt%	Agglomeration of CNTs frequently observed with hot-pressed specimens was significantly reduced, and a relatively uniform distribution of CNTs was obtained. The effective dispersion of CNTs contributed to maintaining the densification of composites and superior mechanical properties
2	CNT reinforced Cu matrix nanocomposites [64]	Molecular level process	SEM, high-resolution TEM, Vickers hardness test, and pin-on-disk type wear tests	Wear loss changes	Reduced to 1/3 of the value of pure Cu matrix	The dispersed CNTs in Cu-matrix nanocomposite retards the peeling of Cu grains during the sliding wear process
3	CNT-coated carbon fiber/polyester composites [117]	CVD and electroless dip coating method	SEM, dynamic mechanical thermal analysis, and single fiber pull out test	Interfacial shear stress	Increases monotonically till a growth time of 20 min and drops abruptly after that	Attributed to the larger contact area and mechanical interlocking between the fiber and matrix due to the presence of CNTs on the fiber surface
4	Carbon fiber/epoxy composites [118]	Resin transfer molding	X-ray and SEM	(i) Formation of transverse cracks (ii) Surface of CF	(i) Significantly reduced (ii) Formation of dense CNT networks on the surfaces of CF, making the morphology of surface crowded and flocky	The mechanism of (localized) energy dissipation through transverse microcracking is replaced by another mechanism that promotes (distributed) damage through fiber debonding
5	Ni–P–CNT composite [86]	CVD, ball milling, and electroless deposition	SEM, AFM, XRD), EDS, and Vickers measurements	Wear and friction behavior	Improves significantly	CNTs act as very intense obstacles to the movement of dislocations through the Ni–P matrix, hindering the occurrence of the plastic deformation
6	B_4C/CNT composites with Al additive [89]	Fabricated by hot pressing using Al additive	FE-SEM	(i) Fracture toughness (ii) Bridging of matrix	(i) Slightly improved by CNT addition, and was ranged between 2.37 and 3.10 MPa $m^{1/2}$ (ii) In the case of the composite containing 10 vol% CNT, the cracks were produced from the tip of the indentation,	

(*Continued*)

Table 4: *Continued*

Sl. no.	Matrix	Method of preparation	Testing method	Property affected	Change observed	Possible reason for change
					and much bridging by the CNT was observed in cracks	
7	CNT-epoxy based composites [119]	Sonication and hot curing	SEM and centrifugal accelerator erosion tester and surface profilometry	Erosive wear resistance	The vertically aligned CNT arrays/epoxy erosion rate is decreased by 30, 27, 20, and 13% at impingement angles of 20, 30, 45, and 90, respectively, compared to neat epoxy	CNT alignment configurations strongly influence the erosion resistance of the composites with identical CNT loading fractions
8	Cu-based composites with Cu-coated $NbSe_2$ and CNT [120]	Powder metallurgy technique	SEM and a multi-functional friction and wear tester	(i) Friction coefficient (ii) Wear rate	(i) Increases slightly (ii) Decreases with the increasing content of copper-coated CNT from 1 to 3 wt%. When the range of copper-coated CNT reaches 4 wt%, the wear of copper-based composite increases	$NbSe_2$ with laminated structure significantly improved the friction-reducing property, while CNT with superior mechanical strength enhanced the wear resistance by increasing the load-carrying capacity
9	CNTs with epoxy resin and carbon fiber composites [121]	Ultrasound mixing and sonication. The hardener was then added to the modified resin and mixed using a mechanical agitator for about 10 min. The mixture was degassed in vacuum for 10 min. Finally, the mixture was transferred to open silicone rubber molds and cured for 2 h at 60°C	SEM and Vickers hardness tester	Erosion rate	50% decrease at high impact angles, slight increase at low impact angles	A positive synergy between the carbon fibers and the CNTs, which resulted in a reduced amount of broken and detached fibers in the case of CFRPs
10	MWCNT and polyurethane (PU) [122]	The substrates were cleaned in an ultrasonic bath with acetone for 10 min, air-dried, and subsequently coated with PU coatings. The prepared coating samples were cured at room temperature overnight and were then postcured at 80°C for 1 h in an oven	Electrochemical impedance spectroscopy, polarization curve measurement, salt spray tests, pull-off tests, and dynamic mechanical analysis	Corrosion resistance and adhesion strength	Enhanced by adding 0.4 wt% CNTs. When CNTs rose to 1 wt %, the corrosion rate of the coating increased	Adding CNTs modified the physical properties of the PU coating so that the internal stress induced in the layer–substrate interface attributable to temperature variations during the curing process could be relaxed and reduced

(*Continued*)

Table 4: *Continued*

Sl. no.	Matrix	Method of preparation	Testing method	Property affected	Change observed	Possible reason for change
11	TiC-modified CNT-reinforced Al [99]	Ultrasonication, wet milling, and tip sonication	XRD and high-resolution TEM	Mean friction coefficient and wear weight loss	A reduction of around 68 and 61% in mean friction coefficient as well as a reduction of about 88 and 84.5% in wear weight loss was achieved for 1.5 wt% modified-CNT/Al composite compared to pure Al and 1.5 wt% unmodified sample, respectively	Nanotubes can fill microvoids of the metal particles

composite coatings display remarkable wear resistance and are universally used for applications based on tribological performance [76]. Moreover, incorporating CNTs into cementitious composites makes them suitable for piezoresistive and crack sensors. They can also be a heating composite for deicing on the roads and applied to an accelerated curing method for the cementitious materials in cold weather conditions [143]. The enhanced thermal conductivity qualifies them to be used as heat interface materials and for heat enhancement applications [102]. MWCNT/polymer composites can be used as strain sensors, as their piezoresistive sensitivity is 3.5 times higher than that of a conventional metallic strain gage [144]. Multifunctional CNT yarn reinforced components can be 3D printed and employed in adaptive structures and structural health monitoring [43]. CNT/TPU filaments can also be 3D printed for direct manufacturing of multi-axial force sensors [44]. CNTs incorporated with a mesoporous TiO_2 film on a titanium foil find dye-sensitized solar cells [29]. At low concentrations, epoxy resin-based CFRP with a surface coating of CNTs demonstrates improved energy concentration [145]. Incorporating ZnO and CNTs in a PANI matrix creates nanocomposites that can be employed in solar cells and other energy-related devices [146]. The high aspect ratio of CNTs, high elastic modulus, and strength make them appropriate for fabricating sports goods and energy [147]. Insertion of CNTs can reduce fuel consumption and greenhouse gas consumption by 16% and 26%, respectively [98]. Flexible organic and perovskite solar cells can be manufactured using PEDOT: PSS and CNTs [148]. For light shuttering applications, electrically switchable light absorbers can be fabricated by dye and MWCNTs-doped liquid crystal droplets [149]. CNTs/PLA composites are also implemented in scaffolds for tissue, water treatment, textile, packaging, and even flexible electronic devices [85].

6 Conclusion

The presented review illustrates the basics of CNTs, how they can be fabricated and processed, and the obstacles encountered when they are manufactured. Ball milling seems to be one of the most popular and efficient techniques currently in use, as it gives homogeneous dispersion of CNTs in the metal matrix. The review also demonstrates an extensive study highlighting how different properties of these composites can be observed and experimentally analyzed. Techniques such as SEM, TEM, X-ray spectroscopy, and nanoindentation are commonly used to study and

Table 5: Raman and XRD spectrum analysis

Sl. no	Matrix	Method of preparation	Testing method	Property affected	Change observed	Possible reason for change
1	MWCNTs/polymer nanocomposites [123]	Sonication followed by melt bending	SEM and Raman spectroscopy	Raman spectra	Raman spectroscopy shows 3 prominent bands – G band at 1,580 cm^{-1}, the D band at 1,360 cm^{-1}, and the D' band at 1,620 cm^{-1} with a considerable reduction in the *R* values	Intermolecular interactions and internal stresses
2	Self-sensing MWCNTs/polymers nanocomposites [115]	Hot pressing technique	SEM and Raman spectroscopy	Raman spectra	Sample containing 2.0 wt% MWCNT shows a Raman shift of 0.13, 0.24, and 0.31% when compared with the filled 1.5, 1.0, and 0.5 wt% MWCNTs samples	Strong interfacial interaction between the MWCNTs and the phenolic
3	CNT/polymers composites [124]	Fused filament fabrication and melt mixing	SEM and Raman spectroscopy	Raman spectra	Two characteristic "D" and "G" were found in the Raman spectra	G-band peaks are obtained due to strong interfacial interaction between MWCNTs and the matrix material
4	CNTs grown CFRP matrix composites [125]	Thermal CVD	SEM, HRTEM, and Raman spectroscopy	Raman spectra	The sample shows "D" and "G" bands with D peak centered at 1,334 cm^{-1} and G peak centered at 1,581 cm^{-1}	Disordered carbon and graphite as carbon nanofibers and CNTs
5	Self-sensing nanocomposites [126]	Direct mixing method	SEM and XRD	Diffraction pattern	Matrix with 2.0 wt% of MWCNTs shows higher diffraction peaks compared to the pure sample	Diffraction peaks in the pure sample are due to the short-range regular ordered structure and amorphous disordered structure

estimate the properties of the composite. Their excellent mechanical, thermal, tribological, and electrical properties make them a strong candidate as reinforcement materials, and they find use in all kinds of industries, including aerospace, electronics, and biomedical. Over the past decades, there has been considerable improvement in the manufacturing and synthesis of CNTs, but several areas still require significant research, such as structure control and growth techniques. Advancement in these areas will have essential impacts on the applications of CNTs and will also reduce the cost of fabrication. Tackling the challenges outlined in the article, such as improper bonding at matrix interface, delamination of composites, and ineffective dispersion of CNTs will further streamline the CNT-composite processing, and thereby, their utilization in different industries.

Acknowledgments: The authors would like to thank Universiti Putra Malaysia for financial support through the Geran Putra Berimpak, GPB 9668200. The authors would also like to acknowledge the Department of Aerospace Engineering, Faculty of Engineering, Universiti Putra Malaysia for the close collaboration in this research. The authors are thankful for Vellore Institute of Technology (VIT), Vellore, India for providing seed grant (SG20210290) for conducting preliminary research work.

Funding information: This work was supported by Universiti Putra Malaysia through the Geran Putra Berimpak, GPB 9668200.

Author contributions: All authors have accepted responsibility for the entire content of this manuscript and approved its submission.

Conflict of interest: Authors state no conflict of interest.

Data availability statement: Data sharing is not applicable to this article as no datasets were generated or analyzed during the current study.

References

[1] Dresselhaus MS, Avouris P. Introduction to carbon materials research. Carbon Nanotubes. 2001;50:1–9.
[2] Kroto HW, Heath JR, O'Brien SC, Curl RF, Smalley RE. C60: buckminsterfullerene. Nature. 1985 Nov;318(6042):162–3.
[3] Iijima S. Helical microtubules of graphitic carbon. Nature. 1991 Nov;354(6348):56–8.
[4] Qiu H, Yang J. Structure and properties of carbon nanotubes. Industrial applications of carbon nanotubes. Elsevier; 2017 Jan 1. p. 47–69.
[5] Ibrahim KS. Carbon nanotubes-properties and applications: a review. Carbon Lett. 2013;14(3):131–44.
[6] Thostenson ET, Ren Z, Chou TW. Advances in the science and technology of carbon nanotubes and their composites: a review. Compos Sci Technol. 2001 Oct 1;61(13):1899–912.
[7] Baughman RH, Zakhidov AA, De Heer WA. Carbon nanotubes – the route toward applications. Science. 2002 Aug 2;297(5582):787–92.
[8] Ferreira FV, Franceschi W, Menezes BR, Biagioni AF, Coutinho AR, Cividanes LS. Synthesis, characterization, and applications of carbon nanotubes. In Carbon-based nanofillers and their rubber nanocomposites. Elsevier; 2019 Jan 1. p. 1–45.
[9] Endo M, Strano MS, Ajayan PM. Potential applications of carbon nanotubes. Carbon Nanotubes. 2007;111:13–62.
[10] De Volder MF, Tawfick SH, Baughman RH, Hart AJ. Carbon nanotubes: present and future commercial applications. Science. 2013 Feb 1;339(6119):535–9.
[11] Bandaru PR. Electrical properties and applications of carbon nanotube structures. J Nanosci Nanotechnol. 2007 Apr 1;7(4–5):1239–67.
[12] Rauti R, Musto M, Bosi S, Prato M, Ballerini L. Properties and behavior of carbon nanomaterials when interfacing neuronal cells: How far have we come? Carbon. 2019 Mar 1;143:430–46.
[13] Rathinavel S, Priyadharshini K, Panda D. A review on carbon nanotube: An overview of synthesis, properties, functionalization, characterization, and the application. Mater Sci Eng: B. 2021 Mar 24;268:115095.
[14] Esawi AM, Farag MM. Carbon nanotube reinforced composites: potential and current challenges. Mater Des. 2007 Jan 1;28(9):2394–401.
[15] Geim AK, Novoselov KS. The rise of graphene. Nanosci Technol Collect Rev Nat J. 2010;11–9.
[16] Liang J, Li H, Qi L, Tian W, Li X, Chao X, et al. Fabrication and mechanical properties of CNTs/Mg composites prepared by combining friction stir processing and ultrasonic assisted extrusion. J Alloy Compd. 2017 Dec 25;728:282–8.
[17] Yang K, Yang X, Liu E, Shi C, Ma L, He C, et al. Elevated temperature compressive properties and energy absorption response of *in-situ* grown CNT-reinforced Al composite foams. Mater Sci Eng A. 2017 Apr 6;690:294–302.
[18] Han D, Mei H, Farhan S, Xiao S, Bai Q, Cheng L. Anisotropic compressive properties of CNT/SiC composites produced by direct matrix infiltration of vertically aligned CNT forests. J Alloy Compd. 2017 Apr 15;701:722–6.
[19] Xiong N, Bao R, Yi J, Fang D, Tao J, Liu Y. CNTs/Cu-Ti composites fabrication through the synergistic reinforcement of CNTs and *in situ* generated nano-TiC particles. J Alloy Compd. 2019 Jan 5;770:204–13.
[20] Nadler M, Werner J, Mahrholz T, Riedel U, Hufenbach W. Effect of CNT surface functionalisation on the mechanical properties of multi-walled carbon nanotube/epoxy-composites. Compos Part A Appl Sci Manuf. 2009 Jul 1;40(6–7):932–7.
[21] Mindivan H, Efe A, Kosatepe AH, Kayali ES. Fabrication and characterization of carbon nanotube reinforced magnesium matrix composites. Appl Surf Sci. 2014 Nov 1;318:234–43.
[22] Pan Y, Xiao S, Lu X, Zhou C, Li Y, Liu Z, et al. Fabrication, mechanical properties and electrical conductivity of Al_2O_3

reinforced Cu/CNTs composites. J Alloy Compd. 2019 Apr 25;782:1015–23.
[23] Wu Y, Kim GY, Russell AM. Mechanical alloying of carbon nanotube and Al6061 powder for metal matrix composites. Mater Sci Eng A. 2012 Jan 15;532:558–66.
[24] Murugesan R, Gopal M, Murali G. Effect of Cu, Ni addition on the CNTs dispersion, wear and thermal expansion behavior of Al-CNT composites by molecular mixing and mechanical alloying. Appl Surf Sci. 2019 Nov 30;495:143542.
[25] Devadiga U, Shetty SK, Fernandes P. Assessment of carbon nanotubes (CNTs) and fly ashes (FAs) reinforced Al nano-composites properties synthesised by powder metallurgy. Mater Today Proc. 2020 Jan 1;22:2247–54.
[26] Meng X, Liu T, Shi C, Liu E, He C, Zhao N. Synergistic effect of CNTs reinforcement and precipitation hardening in *in-situ* CNTs/Al–Cu composites. Mater Sci Eng A. 2015 May 1;633:103–11.
[27] Akbarpour MR, Pouresmaeil A. The influence of CNTs on the microstructure and strength of Al-CNT composites produced by flake powder metallurgy and hot pressing method. Diam Relat Mater. 2018 Sep 1;88:6–11.
[28] Chen B, Li S, Imai H, Jia L, Umeda J, Takahashi M, et al. Carbon nanotube induced microstructural characteristics in powder metallurgy Al matrix composites and their effects on mechanical and conductive properties. J Alloy Compd. 2015 Dec 5;651:608–15.
[29] Lee ES, Lee KM, Yoon SI, Ko YG, Shin DH. Influence of CNT incorporation on the photovoltaic behavior of TiO_2 films formed by high-voltage electrophoretic deposition. Curr Appl Phys. 2013 Jul 20;13:S26–9.
[30] Shetty V, Patil BJ. Evaluation of the mechanical properties and microstructure analysis of heat treated LM-12 alloy with SiO_2 and CNT hybrid metal matrix composites. Mater Today: Proc. 2021 Jan 1;46:2880–3.
[31] Alladi A, Aluri M, Maddela N, Abbadi CR. Recent progress of CNTs reinforcement with metal matrix composites using friction stir processing. Mater Today: Proc. 2021 Jan 1;44:1731–8.
[32] Patil A, Nartu MS, Ozdemir F, Banerjee R, Gupta RK, Borkar T. Strengthening effects of multi-walled carbon nanotubes reinforced nickel matrix nanocomposites. J Alloy Compd. 2021 Sep 25;876:159981.
[33] Zare H, Jahedi M, Toroghinejad MR, Meratian M, Knezevic M. Compressive, shear, and fracture behavior of CNT reinforced Al matrix composites manufactured by severe plastic deformation. Mater Des. 2016 Sep 15;106:112–9.
[34] Duan B, Zhou Y, Wang D, Zhao Y. Effect of CNTs content on the microstructures and properties of CNTs/Cu composite by microwave sintering. J Alloy Compd. 2019 Jan 15;771:498–504.
[35] Liu L, Bao R, Yi J, Li C, Tao J, Liu Y, et al. Well-dispersion of CNTs and enhanced mechanical properties in CNTs/Cu-Ti composites fabricated by Molecular Level Mixing. J Alloy Compd. 2017 Dec 5;726:81–7.
[36] Yu B, Zhao Z, Fu S, Meng L, Liu Y, Chen F, et al. Fabrication of PLA/CNC/CNT conductive composites for high electromagnetic interference shielding based on Pickering emulsions method. Compos Part A Appl Sci Manuf. 2019 Oct 1;125:105558.
[37] Sun Y, Hou K, Zhang D, Chang S, Ye L, Cao A, et al. High performance carbon nanotube/polymer composite fibers and water-driven actuators. Compos Sci Technol. 2021 Apr 12;206:108676.
[38] Bai T, Xie T. Fabrication and mechanical properties of WC-Al_2O_3 cemented carbide reinforced by CNTs. Mater Chem Phys. 2017 Nov 1;201:113–9.
[39] Balázsi C, Fényi B, Hegman N, Kövér Z, Wéber F, Vértesy Z, et al. Development of CNT/Si_3N_4 composites with improved mechanical and electrical properties. Compos Part B Eng. 2006 Jan 1;37(6):418–24.
[40] Jackson EM, Laibinis PE, Collins WE, Ueda A, Wingard CD, Penn B. Development and thermal properties of carbon nanotube-polymer composites. Compos Part B Eng. 2016 Mar 15;89:362–73.
[41] Zhao M, Meng L, Ma L, Ma L, Yang X, Huang Y, et al. Layer-by-layer grafting CNTs onto carbon fibers surface for enhancing the interfacial properties of epoxy resin composites. Compos Sci Technol. 2018 Jan 18;154:28–36.
[42] Yavas B, Sahin F, Yucel O, Goller G. Effect of particle size, heating rate and CNT addition on densification, microstructure and mechanical properties of B_4C ceramics. Ceram Int. 2015 Aug 1;41(7):8936–44.
[43] Gardner JM, Sauti G, Kim JW, Cano RJ, Wincheski RA, Stelter CJ, et al. 3-D printing of multifunctional carbon nanotube yarn reinforced components. Addit Manuf. 2016 Oct 1;12:38–44.
[44] Gnanasekaran K, Heijmans T, Van Bennekom S, Woldhuis H, Wijnia S, De With G, et al. 3D printing of CNT-and graphene-based conductive polymer nanocomposites by fused deposition modeling. Appl Mater Today. 2017 Dec 1;9:21–8.
[45] Kim K, Park J, Suh JH, Kim M, Jeong Y, Park I. 3D printing of multiaxial force sensors using carbon nanotube (CNT)/thermoplastic polyurethane (TPU) filaments. Sens Actuators A Phys. 2017 Aug 15;263:493–500.
[46] Zhou X, Deng J, Fang C, Lei W, Song Y, Zhang Z, et al. Additive manufacturing of CNTs/PLA composites and the correlation between microstructure and functional properties. J Mater Sci Technol. 2021 Jan 1;60:27–34.
[47] Gupta V, Alam F, Verma P, Kannan AM, Kumar S. Additive manufacturing enabled, microarchitected, hierarchically porous polylactic-acid/Lithium iron phosphate/carbon nanotube nanocomposite electrodes for high performance Li-Ion batteries. J Power Sources. 2021 May 15;494:229625.
[48] Choudhary S, Islam A, Mukherjee B, Richter J, Arold T, Niendorf T, et al. Plasma sprayed Lanthanum zirconate coating over additively manufactured carbon nanotube reinforced Ni-based composite: Unique performance of thermal barrier coating system without bondcoat. Appl Surf Sci. 2021 Jun 1;550:149397.
[49] Zhou W, Kamata K, Dong M, Nomura N. Laser powder bed fusion additive manufacturing, microstructure evolution, and mechanical performance of carbon nanotube-decorated titanium alloy powders. Powder Technol. 2021 Apr 1;382:274–83.
[50] Yuan S, Zheng Y, Chua CK, Yan Q, Zhou K. Electrical and thermal conductivities of MWCNT/polymer composites fabricated by selective laser sintering. Compos Part A Appl Sci Manuf. 2018 Feb 1;105:203–13.
[51] Liu C, Ding J. Carbon nanotubes reinforced alumina matrix nanocomposites for conductive ceramics by additive manufacturing. Proc Manuf. 2020 Jan 1;48:763–9.

[52] Arif MF, Alhashmi H, Varadarajan KM, Koo JH, Hart AJ, Kumar S. Multifunctional performance of carbon nanotubes and graphene nanoplatelets reinforced PEEK composites enabled *via* FFF additive manufacturing. Compos Part B Eng. 2020 Mar 1;184:107625.
[53] Gonzalez G, Chiappone A, Roppolo I, Fantino E, Bertana V, Perrucci F, et al. Development of 3D printable formulations containing CNT with enhanced electrical properties. Polymer. 2017 Jan 27;109:246–53.
[54] Kasraie M, Abadi PP. Additive manufacturing of conductive and high-strength epoxy-nanocaly-carbon nanotube composites. Addit Manuf. 2021 Jun 10;46:102098.
[55] Delogu F, Gorrasi G, Sorrentino A. Fabrication of polymer nanocomposites *via* ball milling: Present status and future perspectives. Prog Mater Sci. 2017 May 1;86:75–126.
[56] Zhuang S, Lee ES, Lei L, Nunna BB, Kuang L, Zhang W. Synthesis of nitrogen-doped graphene catalyst by high-energy wet ball milling for electrochemical systems. Int J Energy Res. 2016 Dec;40(15):2136–49.
[57] Korotcenkov G, Cho BK. Spray pyrolysis deposition of undoped SnO_2 and In_2O_3 films and their structural properties. Prog Cryst Growth Charact Mater. 2017 Feb 1;63(1):1–47.
[58] Ibrahim MA, Sahin Y, Gidado AY, Said MT. Mechanical properties of aluminium matrix composite including SiC/Al_2O_3 by powder metallurgy-a review. GSJ. 2019 Mar;7(3):23–38.
[59] Chen L, Yao Y. Processing, microstructures, and mechanical properties of magnesium matrix composites: a review. Acta Metal Sin (Engl Lett). 2014 Oct;27(5):762–74.
[60] Dementyeva JN, Kashapov RN, Kashapov NF, Kashapov LN. Disadvantages of the selective laser sintering technology in the manufacture models for investment casting. IOP Conf Series Mater Sci Eng. 2019 Jul 1;570(1):012015. IOP Publishing.
[61] Moore JD, Klemm D, Lindackers D, Grasemann S, Träger R, Eckert J, et al. Selective laser melting of $La(Fe,Co,Si)_{13}$ geometries for magnetic refrigeration. J Appl Phys. 2013 Jul 28;114(4):043907.
[62] Cavaliere P, Sadeghi B, Shabani A. Spark plasma sintering: process fundamentals. InSpark plasma sintering of materials. Cham: Springer; 2019. p. 3–20.
[63] Andrews R, Weisenberger MC. Carbon nanotube polymer composites. Curr Opsolid state Mater Sci. 2004 Jan 1;8(1):31–7.
[64] Esawi AM, Morsi K, Sayed A, Taher M, Lanka SJ. Effect of carbon nanotube (CNT) content on the mechanical properties of CNT-reinforced aluminium composites. Compos Sci Technol. 2010 Dec 31;70(16):2237–41.
[65] Liu ZY, Xiao BL, Wang WG, Ma ZY. Elevated temperature tensile properties and thermal expansion of CNT/2009Al composites. Compos Sci Technol. 2012 Oct 12;72(15):1826–33.
[66] Choi Y, Kim Y, Park SG, Kim YG, Sung BJ, Jang SY, et al. Effect of the carbon nanotube type on the thermoelectric properties of CNT/Nafion nanocomposites. Org Electron. 2011 Dec 1;12(12):2120–5.
[67] Kim MT, Rhee KY, Lee JH, Hui D, Lau AK. Property enhancement of a carbon fiber/epoxy composite by using carbon nanotubes. Compos Part B Eng. 2011 Jul 1;42(5):1257–61.
[68] Liang J, Li H, Qi L, Tian W, Li X, Zhou J, et al. Influence of Ni-CNTs additions on the microstructure and mechanical properties of extruded Mg-9Al alloy. Mater Sci Eng A. 2016 Dec 15;678:101–9.
[69] Li H, Fan J, Geng X, Li B, Liang C, Wang H, et al. Alumina powder assisted carbon nanotubes reinforced Mg matrix composites. Mater Des. 2014 Aug 1;60:637–42.
[70] Ghobadi H, Nemati A, Ebadzadeh T, Sadeghian Z, Barzegar-Bafrooei H. Improving CNT distribution and mechanical properties of MWCNT reinforced alumina matrix. Mater Sci Eng A. 2014 Nov 3;617:110–4.
[71] Peng T, Chang I. Mechanical alloying of multi-walled carbon nanotubes reinforced aluminum composite powder. Powder Technol. 2014 Nov 1;266:7–15.
[72] Hassan EA, Ge D, Zhu S, Yang L, Zhou J, Yu M. Enhancing CF/PEEK composites by CF decoration with polyimide and loosely-packed CNT arrays. Compos Part A Appl Sci Manuf. 2019 Dec 1;127:105613.
[73] Lim DS, You DH, Choi HJ, Lim SH, Jang H. Effect of CNT distribution on tribological behavior of alumina–CNT composites. Wear. 2005 Jul 1;259(1-6):539–44.
[74] Fan Z, Luo G, Zhang Z, Zhou L, Wei F. Electromagnetic and microwave absorbing properties of multi-walled carbon nanotubes/polymer composites. Mater Sci Eng B. 2006 Jul 25;132(1–2):85–9.
[75] Kim KT, Cha SI, Hong SH. Hardness and wear resistance of carbon nanotube reinforced Cu matrix nanocomposites. Mater Sci Eng A. 2007 Mar 25;449:46–50.
[76] Li T, Qu S, Li Z, Tao W, Wang M. Investigation of the mechanical properties of the Ni–P–CNTs coated copper composite materials: Experiments and modeling. Mater Sci Eng A. 2009 Jan 25;500(1–2):182–7.
[77] Wei C, Wang CI, Tai FC, Ting K, Chang RC. The effect of CNT content on the surface and mechanical properties of CNTs-doped diamond like carbon films. Diam Relat Mater. 2010 May 1;19(5–6):562–6.
[78] Lee JH, Rhee KY, Park SJ. The tensile and thermal properties of modified CNT-reinforced basalt/epoxy composites. Mater Sci Eng A. 2010 Oct 15;527(26):6838–43.
[79] Paramsothy M, Chan J, Kwok R, Gupta M. Addition of CNTs to enhance tensile/compressive response of magnesium alloy ZK60A. Compos Part A Appl Sci Manuf. 2011 Feb 1;42(2):180–8.
[80] Kim BJ, Bae KM, Seo MK, An KH, Park SJ. Roles of Ni/CNTs hybridization on rheological and mechanical properties of CNTs/epoxy nanocomposites. Mater Sci Eng A. 2011 Jun 15;528(15):4953–7.
[81] Jin FL, Ma CJ, Park SJ. Thermal and mechanical interfacial properties of epoxy composites based on functionalized carbon nanotubes. Mater Sci Eng A. 2011 Nov 15;528(29–30):8517–22.
[82] Nam DH, Kim YK, Cha SI, Hong SH. Effect of CNTs on precipitation hardening behavior of CNT/Al–Cu composites. Carbon. 2012 Nov 1;50(13):4809–14.
[83] Peng HE, Lü XC, Lin TS, Li HX, Jing AN, et al. Improvement of mechanical properties of Sn–58Bi alloy with multi-walled carbon nanotubes. Trans Nonferrous Met Soc China. 2012 Dec 1;22:s692–6.
[84] Alishahi M, Monirvaghefi SM, Saatchi A, Hosseini SM. The effect of carbon nanotubes on the corrosion and tribological behavior of electroless Ni–P–CNT composite coating. Appl Surf Sci. 2012 Jan 15;258(7):2439–46.

[85] Jun L, Ying L, Lixian L, Xuejuan Y. Mechanical properties and oil content of CNT reinforced porous CuSn oil bearings. Compos Part B Eng. 2012 Jun 1;43(4):1681–6.
[86] Yi XF, Mishra AK, Kim NH, Ku BC, Lee JH. Synergistic effects of oxidized CNTs and reactive oligomer on the fracture toughness and mechanical properties of epoxy. Compos Part A Appl Sci Manuf. 2013 Jun 1;49:58–67.
[87] Kobayashi T, Yoshida K, Yano T. Microstructure, mechanical and thermal properties of B_4C/CNT composites with Al additive. J Nucl Mater. 2013 Sep 1;440(1–3):524–9.
[88] Li CD, Wang XJ, Liu WQ, Shi HL, Ding C, Hu XS, et al. Effect of solidification on microstructures and mechanical properties of carbon nanotubes reinforced magnesium matrix composite. Mater Des. 2014 Jun 1;58:204–8.
[89] Kim WJ, Lee SH. High-temperature deformation behavior of carbon nanotube (CNT)-reinforced aluminum composites and prediction of their high-temperature strength. Compos Part A Appl Sci Manuf. 2014 Dec 1;67:308–15.
[90] Li CD, Wang XJ, Liu WQ, Wu K, Shi HL, Ding C, et al. Microstructure and strengthening mechanism of carbon nanotubes reinforced magnesium matrix composite. Mater Sci Eng A. 2014 Mar 12;597:264–9.
[91] Rashad M, Pan F, Tang A, Asif M, Aamir M. Synergetic effect of graphene nanoplatelets (GNPs) and multi-walled carbon nanotube (MWCNTs) on mechanical properties of pure magnesium. J Alloy Compd. 2014 Aug 5;603:111–8.
[92] Nam TH, Goto K, Yamaguchi Y, Premalal EV, Shimamura Y, Inoue Y, et al. Effects of CNT diameter on mechanical properties of aligned CNT sheets and composites. Compos Part A Appl Sci Manuf. 2015 Sep 1;76:289–98.
[93] Schilde C, Schlömann M, Overbeck A, Linke S, Kwade A. Thermal, mechanical and electrical properties of highly loaded CNT-epoxy composites–A model for the electric conductivity. Compos Sci Technol. 2015 Sep 29;117:183–90.
[94] Rathore DK, Prusty RK, Kumar DS, Ray BC. Mechanical performance of CNT-filled glass fiber/epoxy composite in *in-situ* elevated temperature environments emphasizing the role of CNT content. Compos Part A Appl Sci Manuf. 2016 May 1;84:364–76.
[95] Nam IW, Park SM, Lee HK, Zheng L. Mechanical properties and piezoresistive sensing capabilities of FRP composites incorporating CNT fibers. Composite Struct. 2017 Oct 15;178:1–8.
[96] Faria B, Guarda C, Silvestre N, Lopes JN, Galhofo D. Strength and failure mechanisms of CNT-reinforced copper nanocomposite. Compos Part B Eng. 2018 Jul 15;145:108–20.
[97] Saba F, Haddad-Sabzevar M, Sajjadi SA, Zhang F. The effect of TiC:CNT mixing ratio and CNT content on the mechanical and tribological behaviors of TiC modified CNT-reinforced Al-matrix nanocomposites. Powder Technol. 2018 May 15;331:107–20.
[98] Subadra SP, Yousef S, Griskevicius P, Makarevicius V. High-performance fiberglass/epoxy reinforced by functionalized CNTs for vehicle applications with less fuel consumption and greenhouse gas emissions. Polym Test. 2020 Jun 1;86:106480.
[99] Mohsen MO, Alansari M, Taha R, Senouci A, Abutaqa A. Impact of CNTs' treatment, length and weight fraction on ordinary concrete mechanical properties. Constr Build Mater. 2020 Dec 20;264:120698.
[100] Ding C, Gan W, Hu X, Wu K, Wang X. Investigation into the influence of carbon nanotubes addition on residual stresses and mechanical properties in the CNTs@ SiCp/Mg-6Zn hybrid composite using neutron diffraction method. Mater Sci Eng A. 2020 Oct 21;797:140105.
[101] Wei X, Tao J, Hu Y, Liu Y, Bao R, Li F, et al. Enhancement of mechanical properties and conductivity in carbon nanotubes (CNTs)/Cu matrix composite by surface and intratube decoration of CNTs. Mater Sci Eng A. 2021 Jun 1;816:141248.
[102] Shaikh S, Lafdi K, Silverman E. The effect of a CNT interface on the thermal resistance of contacting surfaces. Carbon. 2007 Apr 1;45(4):695–703.
[103] Du B, Fang Z. Effects of carbon nanotubes on the thermal stability and flame retardancy of intumescent flame-retarded polypropylene. Polym Degrad Stab. 2011 Oct 1;96(10):1725–31.
[104] Kim KT, Choi SY, Shin EH, Moon KS, Koo HY, Lee GG, et al. The influence of CNTs on the thermoelectric properties of a CNT/Bi_2Te_3 composite. Carbon. 2013 Feb 1;52:541–9.
[105] Wang X, Jiang Q, Xu W, Cai W, Inoue Y, Zhu Y. Effect of carbon nanotube length on thermal, electrical and mechanical properties of CNT/bismaleimide composites. Carbon. 2013 Mar 1;53:145–52.
[106] Gorrasi G, Milone C, Piperopoulos E, Pantani R. Preparation, processing and analysis of physical properties of calcium ferrite-CNTs/PET nano-composite. Compos Part B Eng. 2015 Nov 1;81:44–52.
[107] Tan HX, Xu XC. Conductive properties and mechanism of various polymers doped with carbon nanotube/polyaniline hybrid nanoparticles. Compos Sci Technol. 2016 May 18;128:155–60.
[108] Abdelrazek EM, Elashmawi IS, Hezma AM, Rajeh A, Kamal M. Effect of an encapsulate carbon nanotubes (CNTs) on structural and electrical properties of PU/PVC nanocomposites. Phys B Condens Matter. 2016 Dec 1;502:48–55.
[109] Bairan A, Selamat MZ, Sahadan SN, Malingam SD, Mohamad N. Effect of carbon nanotubes loading in multifiller polymer composite as bipolar plate for PEM fuel cell. Proc Chem. 2016 Jan 1;19:91–7.
[110] Gupta P, Rajput M, Singla N, Kumar V, Lahiri D. Electric field and current assisted alignment of CNT inside polymer matrix and its effects on electrical and mechanical properties. Polymer. 2016 Apr 20;89:119–27.
[111] Peng B, Takai C, Razavi-Khosroshahi H, Salmawy ME, Fuji M. Effect of CNTs on morphology and electromagnetic properties of non-firing CNTs/silica composite ceramics. Adv Powder Technol. 2018 Aug 1;29(8):1865–70.
[112] Kong L, Yin X, Xu H, Yuan X, Wang T, Xu Z, et al. Powerful absorbing and lightweight electromagnetic shielding CNTs/RGO composite. Carbon. 2019 Apr 1;145:61–6.
[113] Thi TB, Ata S, Morimoto T, Okazaki T, Yamada T, Hata K. Visualizing electrical network in microinjection-molded CNT polycarbonate composite. Carbon. 2019 Nov 1;153:136–47.
[114] Chaturvedi AK, Gupta MK, Pappu A. The role of carbon nanotubes on flexural strength and dielectric properties of water sustainable fly ash polymer nanocomposites. Phys B Condens Matter. 2021 Nov 1;620:413283.
[115] Al-Bahrani M, Bouaissi A, Cree A. Mechanical and electrical behaviors of self-sensing nanocomposite-based MWCNTs material when subjected to twist shear load. Mech Adv Mater Struct. 2021 Jun 23;28(14):1488–97.

[116] Al-Bahrani M, Gombos ZJ, Cree A. Investigation of the constancy of the MWCNTs on the fibres surface for manufactured self-sensing composites. Compos Part B Eng. 2019 Sep 15;173:106998.
[117] Agnihotri P, Basu S, Kar KK. Effect of carbon nanotube length and density on the properties of carbon nanotube-coated carbon fiber/polyester composites. Carbon. 2011 Aug 1;49(9):3098–106.
[118] De Greef N, Gorbatikh L, Godara A, Mezzo L, Lomov SV, Verpoest I. The effect of carbon nanotubes on the damage development in carbon fiber/epoxy composites. Carbon. 2011 Nov 1;49(14):4650–64.
[119] Chen J, Hutchings IM, Deng T, Bradley MS, Koziol KK. The effect of carbon nanotube orientation on erosive wear resistance of CNT-epoxy based composites. Carbon. 2014 Jul 1;73:421–31.
[120] Chen B, Yang J, Zhang Q, Huang H, Li H, Tang H, et al. Tribological properties of copper-based composites with copper coated $NbSe_2$ and CNT. Mater Des. 2015 Jun 15;75:24–31.
[121] Papadopoulos A, Gkikas G, Paipetis AS, Barkoula NM. Effect of CNTs addition on the erosive wear response of epoxy resin and carbon fibre composites. Compos Part A Appl Sci Manuf. 2016 May 1;84:299–307.
[122] Gu BE, Huang CY, Shen TH, Lee YL. Effects of multiwall carbon nanotube addition on the corrosion resistance and underwater acoustic absorption properties of polyurethane coatings. Prog Org Coat. 2018 Aug 1;121:226–35.
[123] Bounos G, Andrikopoulos KS, Karachalios TK, Voyiatzis GA. Evaluation of multi-walled carbon nanotube concentrations in polymer nanocomposites by Raman spectroscopy. Carbon. 2014 Sep 1;76:301–9.
[124] Mora A, Verma P, Kumar S. Electrical conductivity of CNT/polymer composites: 3D printing, measurements and modeling. Compos Part B Eng. 2020 Feb 15;183:107600.
[125] Sharma SP, Lakkad SC. Effect of CNTs growth on carbon fibers on the tensile strength of CNTs grown carbon fiber-reinforced polymer matrix composites. Compos Part A Appl Sci Manuf. 2011 Jan 1;42(1):8–15.
[126] Al-Bahrani M, Cree A. *In situ* detection of oil leakage by new self-sensing nanocomposite sensor containing MWCNTs. Appl Nanosci. 2021 Sep;11(9):2433–45.
[127] Yazdchi K, Salehi M. The effects of CNT waviness on interfacial stress transfer characteristics of CNT/polymer composites. Compos Part A Appl Sci Manuf. 2011 Oct 1;42(10):1301–9.
[128] Dastgerdi JN, Marquis G, Salimi M. The effect of nanotubes waviness on mechanical properties of CNT/SMP composites. Compos Sci Technol. 2013 Sep 24;86:164–9.
[129] Rafiee R. Influence of carbon nanotube waviness on the stiffness reduction of CNT/polymer composites. Composite Struct. 2013 Mar 1;97:304–9.
[130] Hassanzadeh-Aghdam MK, Mahmoodi MJ, Jamali J. Effect of CNT coating on the overall thermal conductivity of unidirectional polymer hybrid nanocomposites. Int J Heat Mass Transf. 2018 Sep 1;124:190–200.
[131] Hassanzadeh-Aghdam MK, Mahmoodi MJ, Jamali J, Ansari R. A new micromechanical method for the analysis of thermal conductivities of unidirectional fiber/CNT-reinforced polymer hybrid nanocomposites. Compos Part B Eng. 2019 Oct 15;175:107137.
[132] Rezaei R, Shariati M, Tavakoli-Anbaran H, Deng C. Mechanical characteristics of CNT-reinforced metallic glass nanocomposites by molecular dynamics simulations. Comput Mater Sci. 2016 Jun 15;119:19–26.
[133] Choi BK, Yoon GH, Lee S. Molecular dynamics studies of CNT-reinforced aluminum composites under uniaxial tensile loading. Compos Part B Eng. 2016 Apr 15;91:119–25. Choi BK, Yoon GH, Lee S. Molecular dynamics studies of CNT-reinforced aluminum composites under uniaxial tensile loading. Composites Part B Eng. 2016 Apr 15;91:119–25.
[134] Hassanzadeh-Aghdam MK, Ansari R, Mahmoodi MJ. Micromechanical estimation of biaxial thermomechanical responses of hybrid fiber-reinforced metal matrix nanocomposites containing carbon nanotubes. Mech Mater. 2018 Apr 1;119:1–5.
[135] Arora G, Pathak H. Modeling of transversely isotropic properties of CNT-polymer composites using meso-scale FEM approach. Compos Part B Eng. 2019 Jun 1;166:588–97.
[136] Miao X, Li C, Jiang Y. Free vibration analysis of metal-ceramic matrix composite laminated cylindrical shell reinforced by CNTs. Composite Struct. 2021 Mar 15;260:113262.
[137] Li T, Li M, Gu Y, Wang S, Li Q, Zhang Z. Mechanical enhancement effect of the interlayer hybrid CNT film/carbon fiber/epoxy composite. Compos Sci Technol. 2018 Sep 29;166:176–82.
[138] Mei H, Fan Y, Yan Y, Han D, Cheng L. Three-dimensional CNT lamellae reinforced SiC for enhanced mechanical and electromagnetic shielding properties. Ceram Int. 2020 Nov 1;46(16):25008–16.
[139] Xu Q, Zhang W. Improvement of the electromechanical properties of thermoplastic polyurethane composite by ionic liquid modified multiwall carbon nanotubes. e-Polymers. 2021 Jan 1;21(1):166–78.
[140] Kim T, Sridharan I, Zhu B, Orgel J, Wang R. Effect of CNT on collagen fiber structure, stiffness assembly kinetics and stem cell differentiation. Mater Sci Eng C. 2015 Apr 1;49:281–9.
[141] Ma PC, Tang BZ, Kim JK. Effect of CNT decoration with silver nanoparticles on electrical conductivity of CNT-polymer composites. Carbon. 2008 Sep 1;46(11):1497–505.
[142] Theilmann P, Yun DJ, Asbeck P, Park SH. Superior electromagnetic interference shielding and dielectric properties of carbon nanotube composites through the use of high aspect ratio CNTs and three-roll milling. Org Electron. 2013 Jun 1;14(6):1531–7.
[143] Kim GM, Park SM, Ryu GU, Lee HK. Electrical characteristics of hierarchical conductive pathways in cementitious composites incorporating CNT and carbon fiber. Cement and Concrete. Composites. 2017 Sep 1;82:165–75.
[144] Oliva-Avilés AI, Avilés F, Seidel GT, Sosa V. On the contribution of carbon nanotube deformation to piezoresistivity of carbon nanotube/polymer composites. Compos Part B Eng. 2013 Apr 1;47:200–6.
[145] Weidt D, Figiel Ł. Effect of CNT waviness and van der Waals interaction on the nonlinear compressive behaviour of epoxy/CNT nanocomposites. Compos Sci Technol. 2015 Aug 12;115:52–9.

[146] Saadattalab V, Shakeri A, Gholami H. Effect of CNTs and nano ZnO on physical and mechanical properties of polyaniline composites applicable in energy devices. Prog Nat Sci Mater Int. 2016 Dec 1;26(6):517–22.
[147] Prusty RK, Rathore DK, Ray BC. Evaluation of the role of functionalized CNT in glass fiber/epoxy composite at above-and sub-zero temperatures: Emphasizing interfacial microstructures. Compos Part A Appl Sci Manuf. 2017 Oct 1;101:215–26.
[148] Markose KK, Jasna M, Subha PP, Antony A, Jayaraj MK. Performance enhancement of organic/Si solar cell using CNT embedded hole selective layer. Sol Energy. 2020 Nov 15;211:158–66.
[149] Sharma V, Kumar P. Studies of absorption coefficient cum electro-optic performance of polymer dispersed liquid crystal doped with CNT and dichroic dye. Phys B: Condens Matter. 2017 Nov 1;524:118–22.